Title

β-Cell Dysfunctional ERAD/Ubiquitin/Proteasome System in Type 2 Diabetes Mediated by Islet Amyloid Polypeptide–Induced UCH-L1 Deficiency

Journal

Diabetes, 60(1)

ISSN

0012-1797

Authors

Costes, Safia
Huang, Chang-jiang
Gurlo, Tatyana
et al.

Publication Date

2011

DOI

10.2337/db10-0522

Peer reviewed

β-Cell Dysfunctional ERAD/Ubiquitin/Proteasome System in Type 2 Diabetes Mediated by Islet Amyloid Polypeptide–Induced UCH-L1 Deficiency

Safia Costes,[1] Chang-jiang Huang,[1] Tatyana Gurlo,[1] Marie Daval,[1] Aleksey V. Matveyenko,[1] Robert A. Rizza,[2] Alexandra E. Butler,[1] and Peter C. Butler[1]

OBJECTIVE—The islet in type 2 diabetes is characterized by β-cell apoptosis, β-cell endoplasmic reticulum stress, and islet amyloid deposits derived from islet amyloid polypeptide (IAPP). Toxic oligomers of IAPP form intracellularly in β-cells in humans with type 2 diabetes, suggesting impaired clearance of misfolded proteins. In this study, we investigated whether human-IAPP (h-IAPP) disrupts the endoplasmic reticulum–associated degradation/ubiquitin/proteasome system.

RESEARCH DESIGN AND METHODS—We used pancreatic tissue from humans with and without type 2 diabetes, isolated islets from h-IAPP transgenic rats, isolated human islets, and INS 832/13 cells transduced with adenoviruses expressing either h-IAPP or a comparable expression of rodent-IAPP. Immunofluorescence and Western blotting were used to detect polyubiquitinated proteins and ubiquitin carboxyl-terminal hydrolase L1 (UCH-L1) protein levels. Proteasome activity was measured in isolated rat and human islets. UCH-L1 was knocked down by small-interfering RNA in INS 832/13 cells and apoptosis was evaluated.

RESULTS—We report accumulation of polyubiquinated proteins and UCH-L1 deficiency in β-cells of humans with type 2 diabetes. These findings were reproduced by expression of oligomeric h-IAPP but not soluble rat-IAPP. Downregulation of UCH-L1 expression and activity to reproduce that caused by h-IAPP in β-cells induced endoplasmic reticulum stress leading to apoptosis.

CONCLUSIONS—Our results indicate that defective protein degradation in β-cells in type 2 diabetes can, at least in part, be attributed to misfolded h-IAPP leading to UCH-L1 deficiency, which in turn further compromises β-cell viability. ***Diabetes*** **60: 227–238, 2011**

Type 2 diabetes is characterized by a progressive decline in β-cell function in the face of insulin resistance. Although the mechanisms underlying β-cell dysfunction are unknown, it is likely related to the presence of β-cell endoplasmic reticulum (ER) stress (1,2), increased β-cell apoptosis (3,4), and decreased β-cell mass (3,5). The islet in type 2 diabetes is also characterized by amyloid deposits derived from islet amyloid polypeptide (IAPP) (3). Insulin resistance, the most important risk factor for development of type 2 diabetes, induces increased β-cell expression of insulin but to an even greater extent IAPP (6,7).

IAPP is a 37–amino acid peptide that is coexpressed and cosecreted with insulin (8). This peptide has the propensity to form amyloid fibrils in species at risk of spontaneously developing diabetes (e.g., nonhuman primates and cats). In contrast, in rodents, IAPP is not amyloidogenic because of proline residue substitutions, and rodents do not spontaneously develop type 2 diabetes with the islet morphology present in humans (9). However, increased expression of human-IAPP (h-IAPP) in rodents may lead to type 2 diabetes with islet pathology comparable to that in humans (10–14). Intracellular IAPP toxic oligomers and ER stress have been reported in β-cells of both humans with type 2 diabetes and rodents with high expression of h-IAPP (1,15,16).

The ER is responsible for synthesis, folding, and maturation of proteins. It is endowed with a quality-control system that facilitates the recognition of misfolded proteins and targets them for degradation by the ubiquitin/proteasome system (17). Efficient removal of misfolded proteins by the endoplasmic reticulum–associated degradation (ERAD) is essential to protect cells from ER stress. This is accomplished by several distinct steps. First, if a protein fails quality control, it is removed from the ER by retrograde translocation. Second, multiple ubiquitin molecules are covalently attached to the targeted protein. Third, the polyubiquinated protein is relocated to the 26S proteasome. Fourth, the ubiquitin chains are removed from the misfolded protein by a deubiquitinating enzyme, and thus it is finally rendered available for degradation by the passage through the 26S proteasome (18).

We recently reported that accumulation of polyubiquitinated proteins occurs in pancreatic islets of h-IAPP transgenic mice but not in mice with comparable transgenic expression of rodent-IAPP (r-IAPP) (16). This implies that increased expression of h-IAPP may interfere with the ERAD/ubiquitin/proteasome system, and thus contribute to β-cell ER stress. β-Cells in type 2 diabetes share many characteristics of neurons in neurodegenerative diseases, such as Alzheimer's and Parkinson's diseases, also characterized by protein misfolding, formation of toxic oligomers of locally expressed amyloidogenic proteins, and proteotoxicity prompting ER stress (9,19). These observations imply that the mechanisms that defend against accumulation of misfolded proteins may be disrupted in β-cells in type 2 diabetes as previously documented in neurodegenerative diseases (19–23). Of interest, impair-

From the [1]Larry Hillblom Islet Research Center, David Geffen School of Medicine, University of California, Los Angeles, Los Angeles, California; and the [2]Endocrine Research Unit, Mayo Clinic and Medical College, Rochester, Minnesota.

Corresponding author: Safia Costes, scostes@mednet.ucla.edu.

Received 12 April 2010 and accepted 14 October 2010. Published ahead of print at http://diabetes.diabetesjournals.org on 27 October 2010. DOI: 10.2337/db10-0522.

ment of the ubiquitin/proteasome pathway has been shown to contribute to neurotoxicity in some neurodegenerative diseases (20–23). In particular, deficiency in ubiquitin carboxyl-terminal hydrolase L1 (UCH-L1) has been observed in the brains of individuals with Alzheimer's and Parkinson's diseases (24). UCH-L1, a member of the deubiquinating enzyme family, is abundantly expressed in β-cells (25) and neurons (26). UCH-L1 is required to hydrolyze ubiquitin chains leading to both the release of protein targeted for degradation from the ubiquitin chain so that it can gain access to the proteasome and the generation of free monomeric ubiquitin that is then available for further cycles of the ubiquitin system. Thus, UCH-L1 deficiency impairs ubiquitin-dependent protein degradation and results in accumulation of highly ubiquitinated proteins (27–29).

Given the parallels between neurons in neurodegenerative diseases and islets in type 2 diabetes, we hypothesized that the ERAD/ubiquitin/proteasome system is compromised in β-cells in type 2 diabetes. Further, we hypothesized that increased expression of amyloidogenic h-IAPP would reproduce this dysfunction. Finally, we postulated that the specific mechanism subserving the compromised ERAD/ubiquitin/proteasome system in β-cells in type 2 diabetes, and as a consequence of increased expression of h-IAPP, is decreased availability of UCH-L1.

RESEARCH DESIGN AND METHODS

Cell culture. Rat insulinoma cell line INS 832/13 was provided by Dr. C. Newgard (Durham, NC) (30). For the transduction experiments, cells were plated on six-well plates at 10^6 cells/well, cultured for 24 h, and transduced with r-IAPP or h-IAPP adenoviruses at 400 multiplicity of infection (MOI) for 48 h. At the end of the experiment, cells were lysed for 30 min at 4°C in a solubilizing buffer (31).

Animal model: pancreas processing and islet isolation. The generation of h-IAPP transgenic rats (HIP rats) has been described previously (10). Rats were bred and housed at the animal housing facility of the University of California Los Angeles (UCLA). The UCLA Institutional Animal Care and Use Committee approved all surgical and experimental procedures. For immunofluorescence, wild-type and HIP rats (2 months old) were randomly assigned to either a high-fat diet (HFD) (60% fat, 20% protein, and 20% carbohydrates; Research Diets, New Brunswick, NJ) or a control regular diet (10% fat, 20% protein, and 70% carbohydrates; Research Diets) and were fed ad libitum for 10 weeks (6) (supplementary Table 3 in the online appendix, available at http://diabetes.diabetesjournals.org/cgi/content/full/db10-0522/DC1). Pancreata were fixed with 4% paraformaldehyde (Sigma), paraffin embedded, and cut into 4-μm sections. Islets were obtained from 4- to 6-month-old wild-type (fasting blood glucose [FBG] 77 ± 4 mg/dl) and prediabetic HIP rats (FBG 87 ± 4 mg/dl) (as described in 16). Islets were lysed in lysis buffer (50 mmol/l HEPES, 1% Nonidet P-40, 2 mmol/l Na_3VO_4, 100 mmol/l NaF, 10 mmol/l $PyrPO_4$, 4 mmol/l EDTA, 1 mmol/l PMSF, 1 μg/ml leupeptin, and 1 μg/ml aprotinin), sonicated for 10 s, centrifuged, and stored at −20°C until use for subsequent protein determination by bicinchoninic acid assay (Bio-Rad, Hercules, CA) and Western blotting.

Human islets. Isolated human islets were obtained from the Islet Cell Resource Consortium (http://icr.coh.org). The islet purity was 90–95%, as assessed by dithizone staining. Islets used for transduction experiments were obtained from nine heart-beating organ donors (five men and four women, 45 ± 15 years of age, BMI 28 ± 5 kg/m^2), and none had a previous history of diabetes or metabolic disorders. Islet viability was 80–95%, as assessed by the live/dead kit (Invitrogen). Islets were transduced with r-IAPP or h-IAPP adenoviruses at 400 MOI for 72 h in RPMI-1640 medium containing 100 units/ml of penicillin, 100 μg/ml of streptomycin, and 10% FBS (Invitrogen). Islets used for analysis of ubiquitin or UCH-L1 expression were obtained from four heart-beating organ donors with type 2 diabetes and three BMI-matched nondiabetic control subjects (supplementary Table 1).

Human pancreatic tissue. Institutional review board approval was obtained from the Mayo Clinic (no. 1516-03) and UCLA (no. 06-04-021-01). We obtained human pancreatic tissue at autopsy from 6 lean nondiabetic subjects, 10 obese subjects with type 2 diabetes, and 5 BMI-matched nondiabetic control subjects (supplementary Table 2). Pancreas samples from subjects with type 2 diabetes were from individuals who had been treated with diet alone and/or sulfonylurea treatment (FBG 172 ± 26 mg/dl) or diet and insulin therapy (FBG 213 ± 49 mg/dl). Pancreatic sections were stained with an anti-ubiquitin antibody and stained in parallel for insulin to identify β-cells. We obtained nontumor-involved pancreatic tissue following surgical pancreatectomy for pancreatic tumors from three nondiabetic humans and three obese humans with type 2 diabetes (supplementary Table 4). Pancreas was processed as previously described (1).

Western blotting. Proteins (25–50 μg/lane) were separated on a 4–12% Bis-Tris NuPAGE gel and blotted onto a nitrocellulose membrane (Whatman, Germany). Membranes were probed overnight at 4°C with primary antibodies against Poly (ADP-ribose) polymerase (PARP), phospho-eIF2-α (Ser51), β-actin, glyceraldehyde 3-phosphate dehydrogenase (GAPDH), and ubiquitin from Cell Signaling Technology (Beverly, MA); human ubiquitin from R&D Systems; ubiquitin (clone FK2) from Biomol International (Plymouth Meeting, PA); UCH-L1 from Chemicon International (Temecula, CA); β-tubulin from Sigma; C/EBP homologous protein (CHOP) from Santa Cruz Biotechnology (Santa Cruz, CA); IAPP (25–37 aa) from Peninsula Laboratories (San Carlos, CA); and insulin from Zymed Laboratories (San Francisco, CA). For detection of apoptosis, membranes were probed with an antibody against the cleaved form of caspase-3 (Cell Signaling Technology). We consider cleaved caspase-3 as a reliable marker because a variety of alternative approaches have been previously used in line with cleaved caspase-3 to support emergence of apoptosis in the same models (1,6,32). Horseradish peroxidase–conjugated secondary antibodies were from Zymed Laboratories. Proteins were visualized by enhanced chemiluminescence (Millipore), and protein expression levels were quantified using the Labworks software (UVP, Upland, CA).

Proteasome activity assay. Proteasome activity was assessed using the 20S proteasome activity assay kit (Chemicon International) according to the manufacturer's protocol. Detection was made by spectrofluorometry (BioTek Flx800), with excitation and emission wavelengths at 380 and 460 nm, respectively. The optical density values were normalized to the protein content.

UCH-L1 siRNA. UCH-L1 expression was silenced in INS 832/13 cells using 25-nucleotide stealth-prevalidated siRNA duplexes designed for rat UCH-L1 (Invitrogen). Cells were seeded in 12-well plates and grown overnight to reach 40–50% confluency. The next day, lipofectAMINE2000-siRNA complexes were prepared according to the manufacturer's instructions. UCH-L1 siRNA duplexes were tested at final concentrations of 25 (0.12 μg), 50 (0.24 μg), or 100 nmol/l (0.48 μg). Cells were transfected with UCH-L1 siRNA or control siRNA (scramble) in Opti-MEM (Invitrogen) for 6 h before switching to fresh culture medium; cells were lysed 24, 48, or 72 h after transfection.

Immunofluorescent staining. INS 832/13 cells were plated in four-well chamber permanox slides (Nunc, Rochester, NY) at 100,000 cells per well. After the treatment (as indicated), the immunofluorescence procedure was performed as described in 33. Cells were incubated overnight at 4°C with anti-CHOP antibody, followed by a 1-h treatment with secondary antibody conjugated to Cy3 (Jackson ImmunoResearch Laboratories, West Grove, PA). Slides were viewed using a Leica DM6000 microscope (Leica Microsystems, Bannockburn, IL) and imaged using Openlab software (Improvision, Lexington, MA). The immunofluorescence of rat and human tissues was as described (1).

Image analysis. For detailed evaluation of β-cells positive for ubiquitin, 15 islets per case were selected randomly. The β-cell was considered to be positive if it had any labeling with intensity above background staining of exocrine pancreas. For the quantification of CHOP immunostaining, images of six randomly chosen fields were taken at ×10 magnification. The cells containing nuclear CHOP labeling with intensity above background and the total number of cells in each field were counted. Results were expressed as the percentage of CHOP-positive cells.

Statistical analysis. Results are expressed as the means ± SE for n independent experiments, as indicated in figure legends. Statistical analyses were carried out by Student t test or ANOVA followed by Fisher post hoc test for multiple comparisons using Statistica (Statsoft, Tulsa, OK). A P value of <0.05 was taken as evidence of statistical significance ($^*P < 0.05$; $^{**}P < 0.01$; $^{***}P < 0.001$).

RESULTS

Accumulation of polyubiquitinated proteins in β-cells of humans with type 2 diabetes abrogated by insulin therapy. To test the hypothesis that the ERAD/ubiquitin/proteasome system is dysfunctional in type 2 diabetes, we first examined pancreatic tissue and isolated islets from humans with type 2 diabetes versus BMI-matched control subjects (supplementary Tables 1 and 2). The percentage of β-cells immunostained for ubiquitin was un-

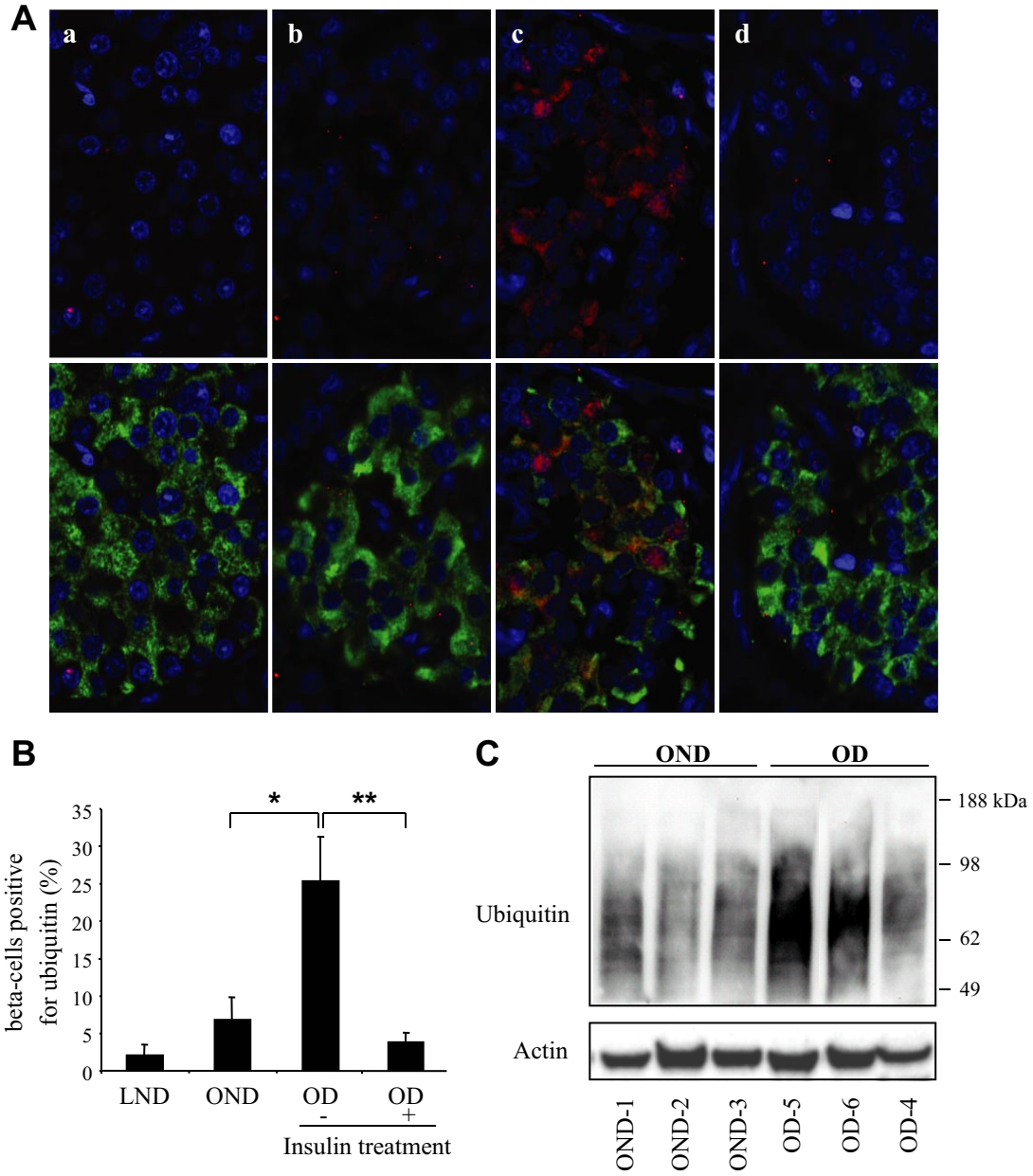

FIG. 1. Accumulation of polyubiquitinated proteins in β-cells of humans with type 2 diabetes abrogated by insulin therapy. *A*: The detection and localization of ubiquitinated proteins was assessed by immunofluorescence (ubiquitin, red; insulin, green; nuclei, blue) in human pancreatic tissue obtained at autopsy from lean nondiabetic (*a*), obese nondiabetic (*b*), obese subjects with type 2 diabetes treated with diet and/or oral medications (nontreated with insulin) (*c*), and obese subjects with type 2 diabetes treated with insulin (*d*). *B*: Percentage of β-cells positive for ubiquitin in each group. LND, lean nondiabetic; OD, obese subjects with type 2 diabetes; OND, obese nondiabetic. Data are expressed as means ± SE. *$P < 0.05$; **$P < 0.01$. *C*: Accumulation of polyubiquitinated proteins was assessed by Western blot in islets isolated from obese nondiabetic and obese subjects with type 2 diabetes. Actin was used as loading control. Ubiquitin and actin images were obtained by grouping different parts of the same gel. (A high-quality digital representation of this figure is available in the online issue.)

changed by obesity in nondiabetic individuals (6.8 ± 2.9% vs. 2.1 ± 1.3%, P = NS, obese nondiabetic vs. lean nondiabetic) (Fig. 1*A* and *B*), implying that in health, the β-cell ERAD/ubiquitin/proteasome system adapts to the increased synthetic burden of insulin and IAPP prompted by obesity-mediated insulin resistance (6,7). In contrast, the percentage of β-cells with ubiquitin immunostaining was increased (approximately fourfold) in obese individuals with type 2 diabetes treated with diet and/or sulfonylureas in comparison to obese nondiabetic individuals (25 ± 6% vs. 6.8 ± 2%, $P < 0.05$) (Fig. 1*A* and *B*). Ubiquitin immunostaining in islets was mostly cytoplasmic, although nuclear staining was also found in some cells, consistent with previous reports documenting the presence of components of the ubiquitin-proteasome pathway in both cytoplasmic and nuclear compartments (34) and implying that defective protein degradation may also alter clearance of nuclear proteins.

Western blot analysis of isolated islets obtained from three individuals with type 2 diabetes and three BMI-matched nondiabetic control subjects (supplementary Table 1) revealed high–molecular weight smears that correspond to polyubiquitinated proteins (Fig. 1*C*). A stronger ubiquitin signal was detected in islets from individuals with type 2 diabetes (Fig. 1*C*), corroborating the increased ubiquitin staining detected by immunohisto-

chemistry of pancreas sections from humans with type 2 diabetes.

Interestingly, we found that the percentage of β-cells positive for ubiquitin in obese individuals with type 2 diabetes treated with insulin was decreased in comparison to individuals treated with diet only or oral sulfonylureas (3.6 ± 1.4% vs. 25 ± 6%, $P < 0.01$) (Fig. 1*A* and *B*), perhaps through the decreased ER synthetic burden mediated by exogenous insulin. IAPP production would be an interesting parameter to follow in this study. Unfortunately, it is not available for these groups of subjects, and relative expression rates can only be inferred from animal studies.

Because accumulation of polyubiquinated proteins in neurodegenerative diseases has been attributed to dysfunction of the ERAD/ubiquitin/proteasome rendered by accumulation of amyloidogenic proteins, we next investigated whether the accumulation of polyubiquitinated proteins in β-cells is induced by increased expression of amyloidogenic h-IAPP.

Pancreatic β-cells from HIP rats display high levels of ubiquitinated proteins associated with decreased UCH-L1 protein expression. We studied 4- to 6-month-old h-IAPP transgenic rats (HIP rat) versus wild-type rats. At this age, HIP rats have increased β-cell apoptosis but do not yet have diabetes, allowing us to avoid the confounding effects of glucose toxicity (RESEARCH DESIGN AND METHODS) (10,14). The percentage of β-cells immunostained for ubiquitin was increased in HIP rats (32 ± 5% vs. 8 ± 5%, $P < 0.01$) (Fig. 2*A* and *B*). The staining was mostly cytoplasmic, although nuclear staining was also evident in some cells (Fig. 2*A*). To draw a parallel between obese individuals with type 2 diabetes and the rat model, we also examined pancreatic sections from HFD-fed HIP rats (6). Within this group of HFD-fed HIP rats, which have diabetes and are insulin resistant, the percentage of β-cells stained for ubiquitin was increased in comparison to HIP rats fed with a regular diet (50 ± 3% vs. 32 ± 5%, $P < 0.05$) (Fig. 2*B*). Ubiquitin immunostaining was predominantly cytoplasmic, although nuclear staining was present in some cells, comparable to islets in type 2 diabetes (Fig. 1*A*). Impaired proteasome function may cause accumulation of ubiquitinated proteins (18). However, proteasome activity was comparable in islets of HIP, HFD-fed HIP, and wild-type rats (Fig. 2*C*).

UCH-L1 permits ubiquitinated proteins to access the proteasome and when deficient may lead to accumulation of polyubiquinated proteins (27–29). Therefore, we next investigated UCH-L1 expression in HIP rat islets. UCH-L1 protein levels were decreased by 42 ± 9% in islets of HIP compared with wild-type rats ($P < 0.01$) (Fig. 3*B*). UCH-L1 mRNA levels were also downregulated by 28 ± 6% in HIP rat islets ($P < 0.05$) (Fig. 3*C*). This downregulation was supported by microarray analysis of HIP versus wild-type rat islets (data not shown). These results suggest that decreased UCH-L1 protein expression occurred, at least in part, at a transcriptional level. Accumulation of ubiquitinated proteins (Fig. 3*A*) and decreased UCH-L1 protein expression were also related to ER stress and apoptosis in HIP rat islets, as shown by increased CHOP expression and increased cleaved caspase-3 respectively (Fig. 3*B*) (6). Also, the frequency of β-cells positive for ubiquitin was highly correlated to β-cell ER stress and β-cell apoptosis ($r = 0.8$, $P < 0.001$, and $r = 0.7$, $P < 0.01$, respectively) (supplementary Fig. 1*A* and *B*). These data suggest that high expression rates of h-IAPP lead to the accumulation of ubiquitinated proteins and downregulation of UCH-L1 in vivo.

h-IAPP but not r-IAPP expression decreases UCH-L1 protein level in β-cells. To establish whether UCH-L1 downregulation is caused by h-IAPP, we studied INS 832/13 cells transduced with adenoviruses expressing h-IAPP or the nonamyloidogenic and nontoxic rodent IAPP (r-IAPP), as control for a comparable burden of protein expression (33). Cells transduced with h-IAPP (400 MOI, 48 h) exhibited a 31 ± 10% decrease in UCH-L1 protein expression in comparison to r-IAPP-transduced cells ($P < 0.05$) (Fig. 4). Therefore, high expression rates of h-IAPP lead to UCH-L1 downregulation in β-cells, and this effect is due to the amyloidogenic properties of h-IAPP rather than just protein overload.

Loss of UCH-L1 function and expression leads to ER stress and β-cell apoptosis. To evaluate whether UCH-L1 downregulation plays a role in the progression of h-IAPP–induced β-cell apoptosis, we treated INS 832/13 cells with UCH-L1 inhibitor, LDN-57444, for 18 h at different concentrations. Inhibition of UCH-L1 function led to increased caspase-3 activity and cleavage at concentrations above 30 μmol/l (Fig. 5*A* and *B*). We next investigated whether apoptosis induced by UCH-L1 inhibitor was related to ER stress. Western blot analysis showed induction of CHOP after exposure to UCH-L1 inhibitor (Fig. 5*B*) and immunostaining revealed that nuclear CHOP was highly induced in LDN-57444–treated cells (13.4 ± 0.4% vs. 2.5 ± 0.8%, $P < 0.01$) (Fig. 5*C*). An increased phosphorylation of eukaryotic initiation factor 2 (eIF2)-α, a target of Perk and ER stress marker, was also detected by Western blot (supplementary Fig. 2*A*).

To further corroborate these findings, we used a siRNA approach to specifically target UCH-L1 and decrease its expression. Transfection of INS 832/13 cells using 25 nmol/l of siRNA resulted in 44 ± 6% knockdown of UCH-L1 protein content (Fig. 6*A* and *B*), reproducing the deficit observed in HIP rat islets (Fig. 3*B*). This decrease in protein content was associated with a decrease in UCH-L1 activity (Fig. 6*A* and *B*), as shown by labeling studies using Ub-VS active site probe for deubiquitinating enzymes. This probe (with an HA tag) covalently modifies active deubiquitinating enzymes in the extracts. Examination of Ub-VS–treated extracts from control or scramble-transfected cells revealed several HA reactive bands, including a 35-kDa band corresponding to UCH-L1 complexed with the probe (35). This band was decreased by ~40% in UCH-L1 siRNA-transfected cells (Fig. 6*A* and *B*), confirming a decrease in active UCH-L1. This decrease in UCH-L1 protein content and activity led to increase of cleaved caspase-3 and of its cleaved substrate PARP (Fig. 6*A* and *B*). Immunostaining revealed that nuclear CHOP was highly induced in UCH-L1–downregulated cells in comparison to scramble-transfected cells (23 ± 3% vs. 6.3 ± 1.3%, $P < 0.01$) (Fig. 6*C*). ER stress was also confirmed by the increase in eIF2-α phosphorylation upon UCH-L1 downregulation (supplementary Fig. 2*B*). In conclusion, chemical inhibition as well as knockdown of UCH-L1 leads to accumulation of ubiquitinated proteins (supplementary Fig. 3), ER stress, and apoptosis in β-cells.

To determine whether a decrease in UCH-L1 exacerbates h-IAPP–induced apoptosis, we transfected INS 832/13 cells with UCH-L1 siRNA or scramble (25 nmol/l, 36 h) and transduced these cells with h-IAPP or r-IAPP adenoviruses at 300 MOI for 30 h. Under these conditions, neither UCH-L1 siRNA nor h-IAPP alone induced cell death as illustrated by cleaved caspase-3 and cleaved

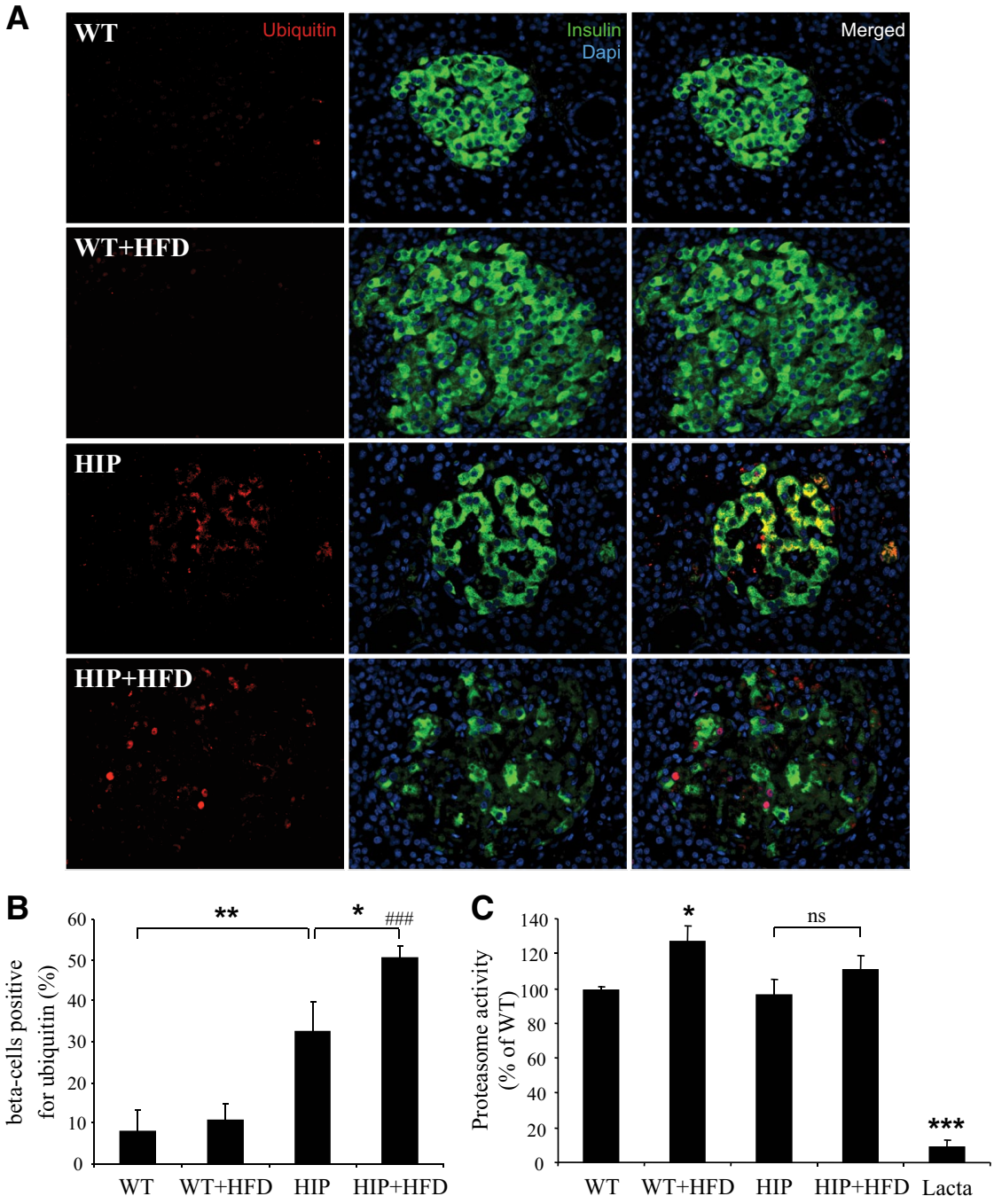

FIG. 2. Accumulation of ubiquitinated proteins in β-cells of HIP rats. *A*: The presence and localization of ubiquitinated proteins were assessed by immunofluorescence (ubiquitin, red; insulin, green; nuclei, blue) in pancreatic tissue obtained from wild-type rats (WT; $n = 4$), wild-type rats on HFD for 10 weeks (WT+HFD; $n = 4$), HIP rats (HIP; $n = 5$), and HIP rats on HFD for 10 weeks (HIP+HFD; $n = 5$). *B*: The graph represents the quantification of β-cells positive for ubiquitin in each group (expressed in percentages). Data are expressed as means ± SE. *$P < 0.05$; **$P < 0.01$; ###$P < 0.001$, significant differences vs. WT+HFD. *C*: Proteasome activity was evaluated in islets isolated from 4- to 6-month-old wild-type rats (WT; $n = 9$), wild-type rats on HFD for 10 weeks (WT+HFD; $n = 4$), HIP rats ($n = 9$), and HIP rats on HFD for 10 weeks (HIP+HFD; $n = 5$). The activity was normalized to the total protein content. The proteasome inhibitor, lactacystin (Lacta; 25 μmol/l) was used as negative control. Data are expressed as means ± SE. *$P < 0.05$; ***$P < 0.001$, significant differences vs. wild type. ns, nonsignificant. (A high-quality digital representation of this figure is available in the online issue.)

PARP levels (supplementary Fig. 4*A* and *B*) or caspase-3 activity (data not shown). UCH-L1 knockdown increased the cleavage of caspase-3 and PARP in both r-IAPP– and h-IAPP–transduced cells in comparison to scramble-transfected cells. However, when UCH-L1 was knocked down in the presence of h-IAPP, cell death was induced to a greater extent in comparison to r-IAPP–transduced cells (supplementary Fig. 4*A* and *B*, *lane 8* vs. *lane 9*, $P < 0.001$). These results demonstrate the critical role of UCH-L1 for β-cell survival under conditions of a high protein synthetic burden.

Increased expression of h-IAPP in isolated human islets leads to accumulation of polyubiquitinated proteins associated with decreased UCH-L1 protein level. To establish whether h-IAPP affects the ubiquitin/proteasome pathway in human β-cells, we transduced

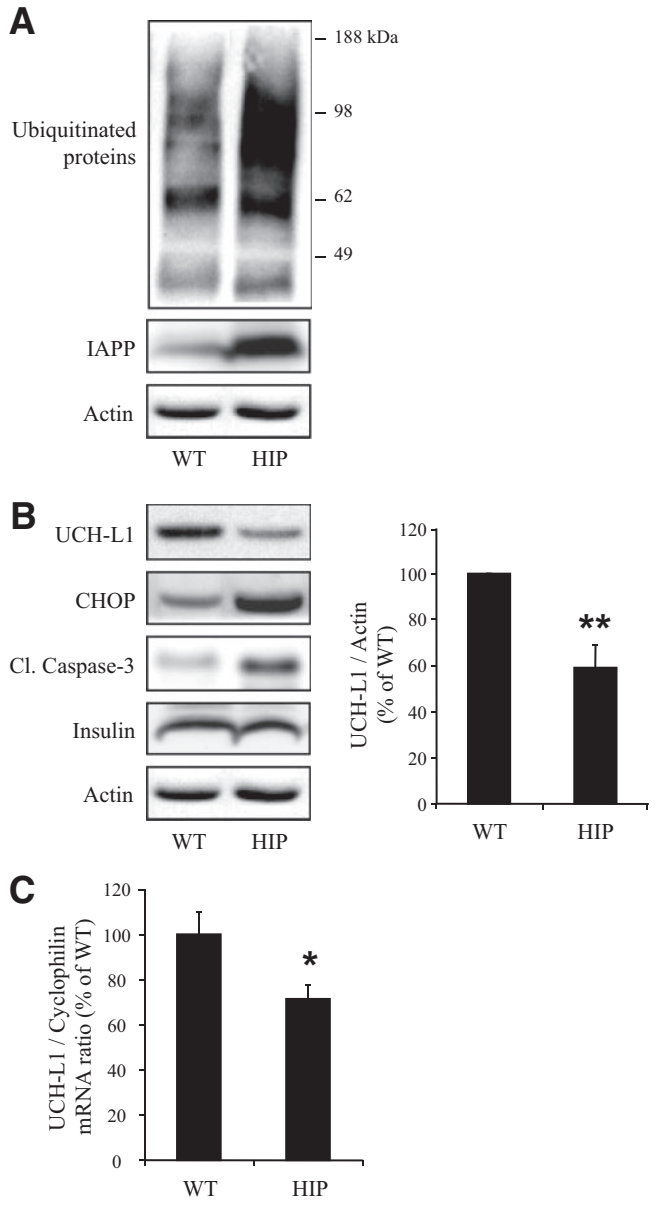

FIG. 3. Expression of h-IAPP decreases UCH-L1 levels in HIP rat islets. *A:* The detection of polyubiquitinated proteins was assessed by Western blot using islet protein lysates obtained from 4- to 6-month-old wild-type (WT; $n = 5$) and HIP rats (HIP; $n = 5$). IAPP and actin were used as control. Ubiquitin image was obtained by grouping different parts of the same gel. *B*: Protein levels of UCH-L1, CHOP, and cleaved caspase-3 (Cl. caspase-3) were assessed by Western blot using islet protein lysates obtained from wild-type ($n = 5$) and HIP ($n = 5$) rats. Insulin and actin were used as control. The graph represents the quantification of UCH-L1 protein levels. *C*: Levels of UCH-L1 mRNA were evaluated by RT-qPCR in islets isolated from wild-type ($n = 9$) and HIP ($n = 9$) rats. Data are expressed as means ± SE. *$P < 0.05$; **$P < 0.01$.

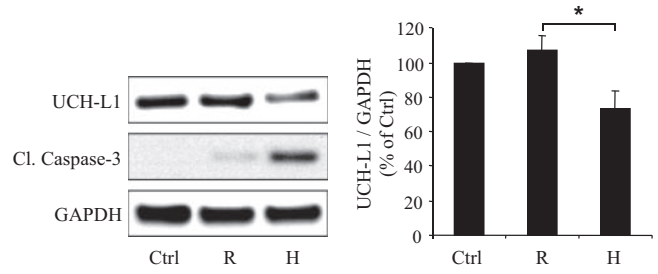

FIG. 4. Expression of h-IAPP, but not r-IAPP, decreases UCH-L1 protein levels in INS 832/13 cells. INS 832/13 cells were transduced at 400 MOI for 48 h with r-IAPP (R) or h-IAPP (H) adenoviruses (Ctrl, nontransduced cells). Protein levels of UCH-L1 and cleaved caspase-3 were analyzed by Western blot. GAPDH was used as loading control. The graph represents the quantification of UCH-L1 protein levels ($n = 4$). Data are expressed as means ± SE. *$P < 0.05$.

isolated human islets with adenoviruses expressing h-IAPP or r-IAPP (400 MOI, 72 h). The accumulation of polyubiquitinated proteins was significantly increased (1.8 ± 0.1-fold, $P < 0.01$) in human islets transduced with h-IAPP, as shown by Western blot analysis (Fig. 7*A*). To address the mechanism by which h-IAPP leads to the accumulation of ubiquitinated proteins in human islets, we examined its actions on proteasome activity as well as on UCH-L1 expression. There was no change in proteasome activity in human islets transduced with h-IAPP in comparison to islets transduced with r-IAPP (Fig. 7*B*). However, overexpression of h-IAPP led to a 40 ± 5% decrease in UCH-L1 protein expression ($P < 0.01$) (Fig. 7*C*), supporting the data obtained in both HIP rat islets (Fig. 3*B*) and INS 832/13 cells (Fig. 4) and suggesting that a specific property of h-IAPP is responsible for accumulation of polyubiquitinated proteins and UCH-L1 downregulation in human β-cells.

UCH-L1 protein level is decreased in β-cells of individuals with obesity and type 2 diabetes. To investigate whether UCH-L1 deficiency occurs in individuals with type 2 diabetes, we examined protein levels in isolated

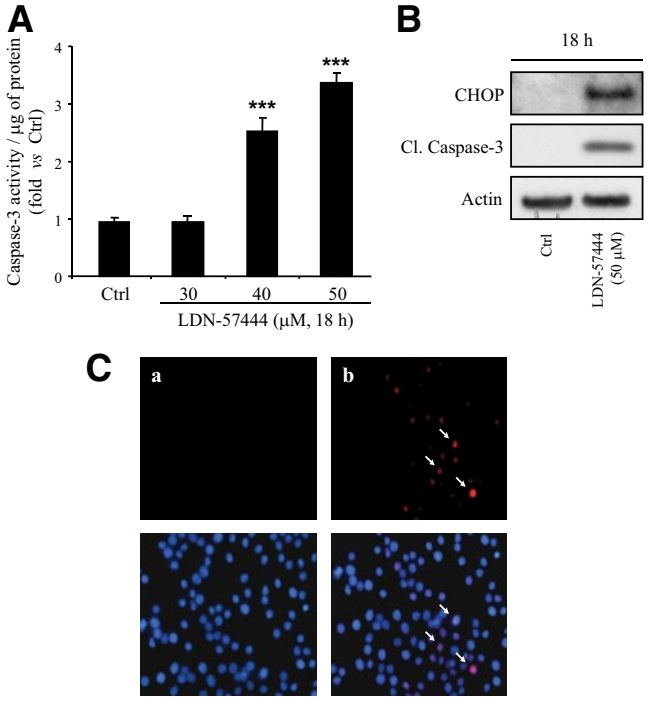

FIG. 5. Inhibition of UCH-L1 activity leads to ER stress and apoptosis in INS 832/13 cells. *A*: INS 832/13 cells were treated for 18 h with UCH-L1 inhibitor, LDN-57444, at increasing concentrations. Apoptosis was assessed by measuring caspase-3 activity in lysates. The activity was normalized to the total protein content. Data are expressed as means ± SE ($n = 4$). ***$P < 0.001$, significant differences vs. cells treated with vehicle DMSO (Ctrl). *B*: INS 832/13 cells were treated or not with LDN-57444 (50 µmol/l) for 18 h. Levels of CHOP and cleaved caspase-3 were analyzed by Western blot. Actin was shown as loading control. *C*: INS 832/13 cells were treated with LDN-57444 (50 µmol/l) for 8 h (*b*) or not treated (*a*). The detection of CHOP (arrows) was assessed by immunofluorescence (CHOP, red; nuclei, blue) ($n = 3$). (A high-quality digital representation of this figure is available in the online issue.)

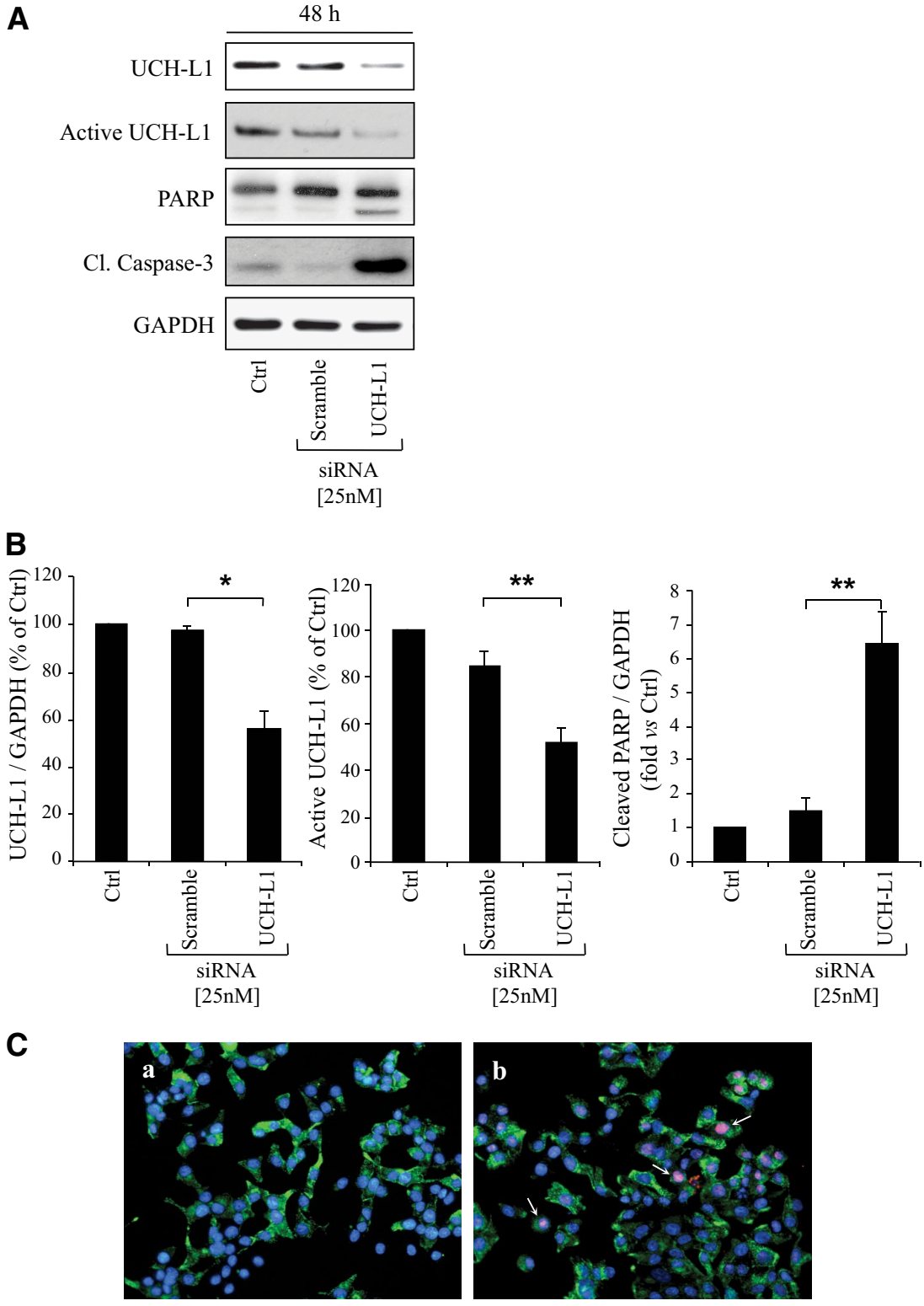

FIG. 6. Downregulation of UCH-L1 by siRNA induces ER stress and apoptosis in INS 832/13 cells. *A*: INS 832/13 cells were transfected for 48 h with scramble or UCH-L1 siRNA (25 nmol/l). Levels of UCH-L1, PARP, and cleaved caspase-3 were analyzed by Western blot. Activity of UCH-L1 was assessed by active-site labeling of deubiquitinating enzymes. The preparations were incubated with HA-Ub-VS and probed with the anti-HA. Levels of GAPDH were shown as loading control. *B*: The graphs represent the quantification of UCH-L1 expression, UCH-L1 activity, and the cleaved form of PARP. Data are expressed as means ± SE (n = 3–4). *P < 0.05; **P < 0.01. *C*: INS 832/13 cells were transfected for 48 h with scramble (*a*) or UCH-L1 siRNA (25 nmol/l) (*b*). The detection of CHOP (arrows) was assessed by immunofluorescence (CHOP, red; insulin, green; nuclei, blue) (n = 3). (A high-quality digital representation of this figure is available in the online issue.)

islets obtained from three obese nondiabetic (OND group) and three obese individuals with type 2 diabetes (OD group) (supplementary Table 1). Western blot analysis of these samples showed decreased UCH-L1 protein levels normalized to β-tubulin in individuals with type 2 diabetes versus BMI-matched nondiabetic control subjects. Insulin

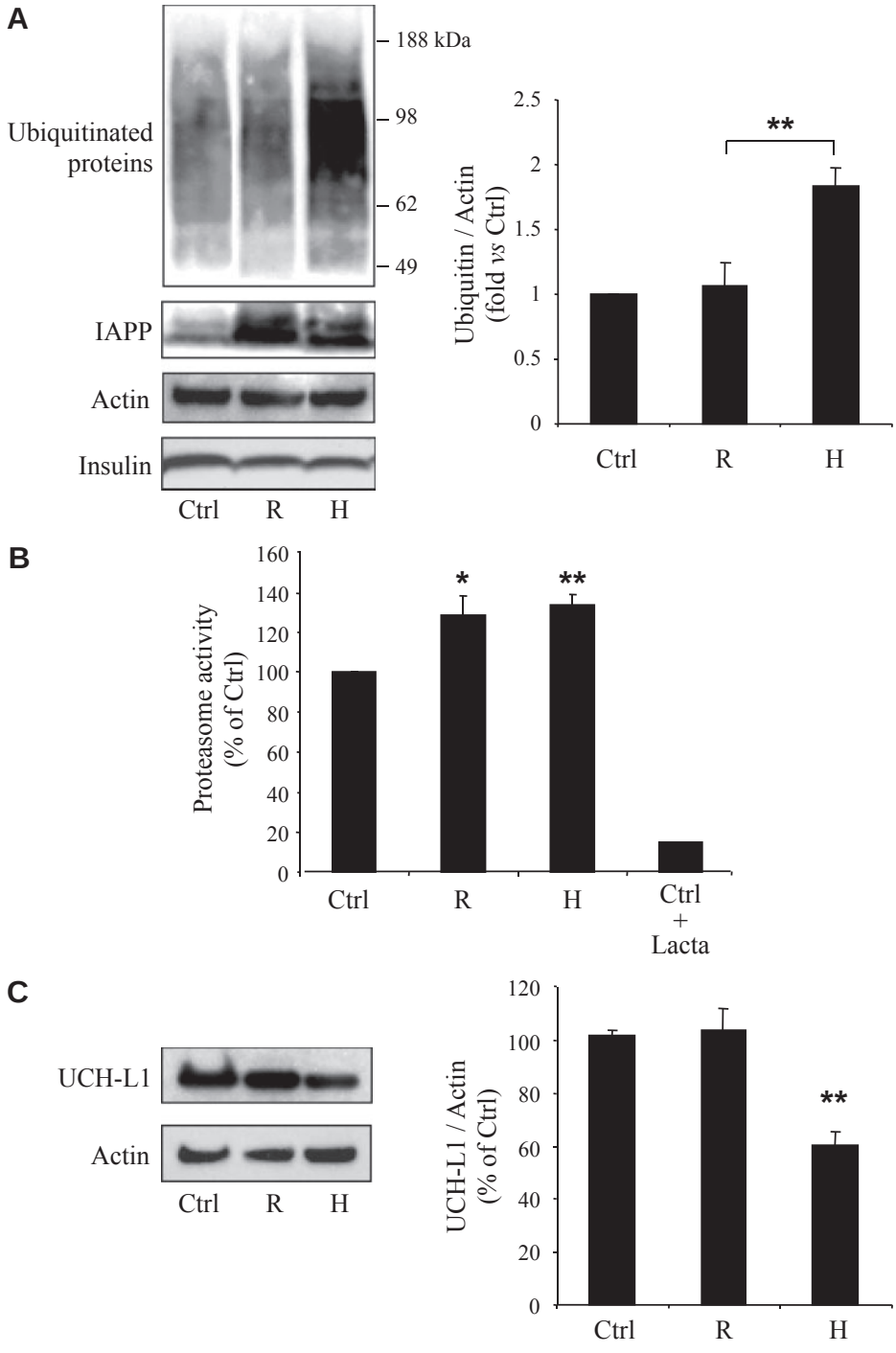

FIG. 7. Expression of h-IAPP in human islets leads to accumulation of polyubiquitinated proteins associated with decrease of UCH-L1. *A*: Human islets were transduced at 400 MOI for 72 h with r-IAPP (R) or h-IAPP (H) adenoviruses. Accumulation of polyubiquitinated proteins and IAPP expression were assessed by Western blot. Insulin and actin were used as control. Ubiquitin and actin images were obtained by grouping different parts of the same gel. The graph represents the quantification of the Western blot ($n = 3$). *B*: Proteasome activity was measured by the 20S proteasome activity assay ($n = 4$). The proteasome inhibitor, lactacystin (Lacta, 25 μmol/l), was used as negative control. *C*: Protein level of UCH-L1 was analyzed by Western blot. Actin was used as loading control. The graph represents the quantification of the Western blot ($n = 3$). Data are expressed as means ± SE. *$P < 0.05$; **$P < 0.01$.

protein levels were also decreased in obese individuals with type 2 diabetes, and this may either reflect diminished number of β-cells per islet and/or depleted insulin stores per β-cell. UCH-L1 protein levels in type 2 diabetes remain decreased even when normalized to insulin (46 ± 14%, $P < 0.05$) (Fig. 8*A*), presumably a conservative estimate of the extent of the deficit.

In addition, analysis of pancreata stained by immunofluorescence for UCH-L1 revealed diminished staining of β-cells in individuals with type 2 diabetes in comparison to nondiabetic individuals (Fig. 8*B*) (supplementary Table 4). These observations support the data obtained by Western blot, indicating that UCH-L1 protein levels are decreased in β-cells of individuals with type 2 diabetes. Interestingly, UCH-L1 protein expression was inversely related to the accumulation of polyubiquitinated proteins in β-cells of

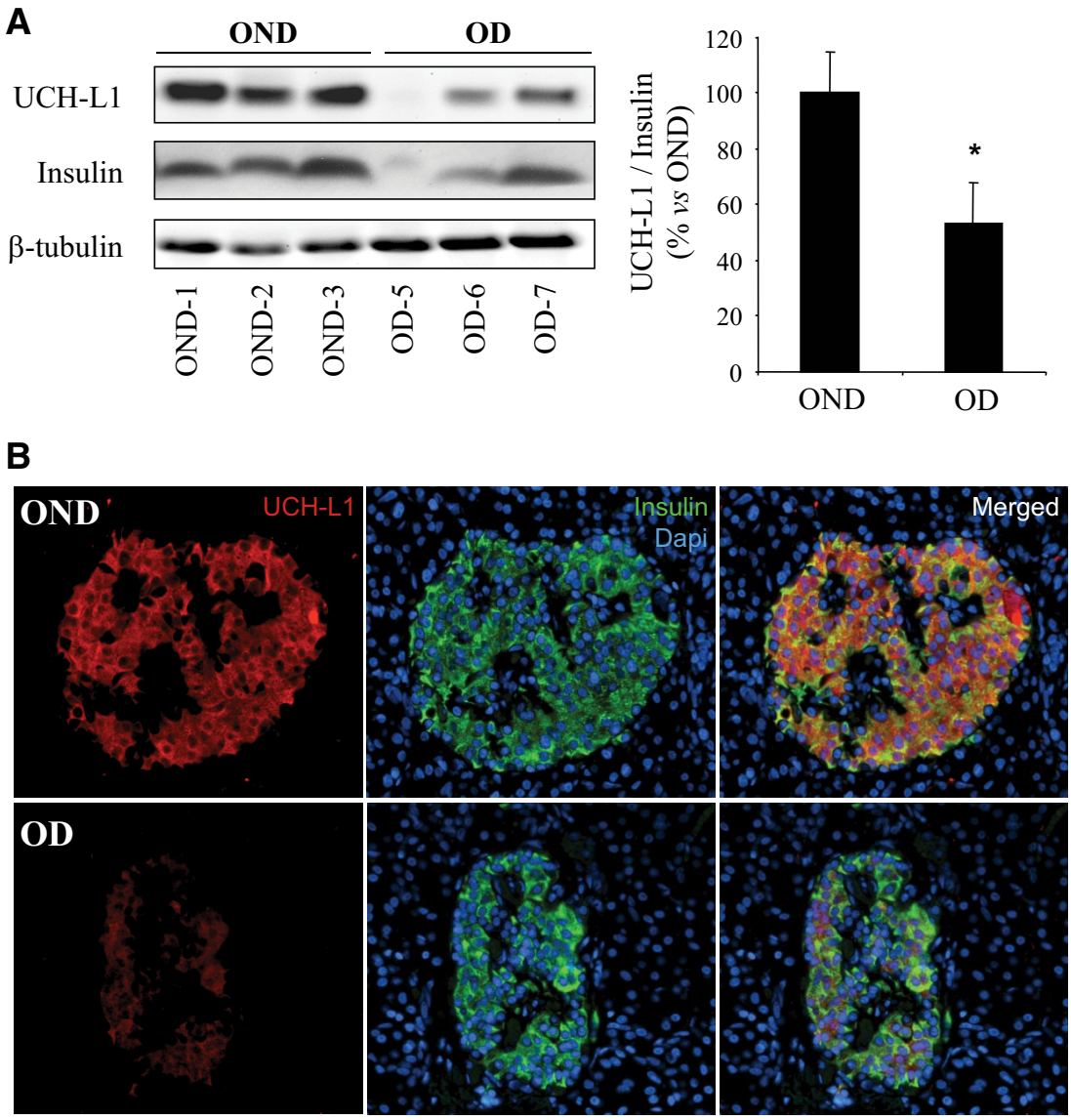

FIG. 8. UCH-L1 deficiency is characteristic to human islets in type 2 diabetes. *A*: UCH-L1 protein expression was analyzed by Western blot in islets isolated from obese nondiabetic (OND) and obese subjects with type 2 diabetes (OD). Levels of β-tubulin and insulin were used as control. The graph represents the quantification of the Western blot. Data are expressed as means ± SE. *$P < 0.05$. *B*: UCH-L1 protein level was assessed by immunofluorescence (UCH-L1, red; insulin, green; nuclei, blue) in surgical pancreatic tissue from obese nondiabetic (OND) and obese subjects with type 2 diabetes (OD). (A high-quality digital representation of this figure is available in the online issue.)

individuals with type 2 diabetes (Fig. 1*C*). Taken together, these data reveal that decreased UCH-L1 availability and accumulation of poyubiquitinated proteins are characteristics of β-cells in type 2 diabetes.

DISCUSSION

We report that the ERAD/ubiquitin/proteasome system is dysfunctional in β-cells of individuals with type 2 diabetes as demonstrated by the accumulation of polyubiquinated proteins. This further supports that islet dysfunction in type 2 diabetes and neuronal dysfunction in neurodegenerative diseases share common mechanisms. In most neurodegenerative diseases, dysfunction of the ERAD/ubiquitin/proteasome system is a consequence of amyloidogenic protein aggregates that, by disrupting this system, further compound their adverse actions (23). An intriguing finding in our studies supports that model. Accumulation of polyubiquinated proteins was decreased in β-cells of individuals with type 2 diabetes treated with insulin therapy in comparison to those treated by sulfonylureas and diet therapy, even though the blood glucose control was comparable. Insulin therapy might thus be expected to protect β-cells against dysfunction of the ERAD/ubiquitin/proteasome system by reducing the synthetic burden for both insulin and IAPP in type 2 diabetes.

Having established that the ERAD/ubiquitin/proteasome system is compromised in β-cells of humans with type 2 diabetes, we sought to examine if this can be reproduced by increased h-IAPP expression. Moreover, we sought to establish if the underlying defect is at the proteasome level or because of decreased UCH-L1 availability. We report that UCH-L1 protein levels are decreased in β-cells of humans with type 2 diabetes, and this is accompanied by accumulation of ubiquitin conjugates. Hyperglycemia, per se, can lead to decreased UCH-L1 expression (25), but our data suggest that h-IAPP misfolding has an independent action on UCH-L1 expression and function. We examined islets from HIP rats at 4 to 6 months of age before this

model develops diabetes but already has β-cell dysfunction (10,14). In those studies, as well as those with isolated human islets and INS 832/13 cells expressing h-IAPP versus r-IAPP, the actions of h-IAPP to compromise UCH-L1 availability were documented independently of glucose toxicity. Moreover, dysfunction of the ERAD/ubiquitin/proteasome system with decreased UCH-L1 availability in neurodegenerative diseases characterized by misfolded amyloidogenic proteins occurs in the absence of diabetes. Therefore, we speculate that the defect in protein degradation apparent in β-cells in type 2 diabetes can, at least in part, be attributed to misfolded h-IAPP leading to UCH-L1 deficiency, which in turn likely further compromises β-cell viability by exacerbating ER stress.

These findings raise the question, how does amyloidogenic h-IAPP lead to decreased UCH-L1 availability? UCH-L1 mRNA and protein expression were decreased in HIP rat islets, but the mechanisms responsible for this downregulation remain to be elucidated. UCH-L1 transcriptional repression was shown to be mediated through CpG hypermethylation of its promoter in renal cells (36). Interestingly, ER stress induces transcriptional repression through promoter hypermethylation (37). Therefore, h-IAPP–mediated ER stress could lead to hypermethylation of the UCH-L1 gene promoter, leading to decreased mRNA and protein levels. Post-transcriptional and post-translational modifications of UCH-L1 might also account for decreased UCH-L1 availability. In neurons from individuals with Alzheimer's or Parkinson's disease, UCH-L1 protein expression is decreased and is also a major target of oxidative damage (24). UCH-L1 is thus extensively modified by carbonyl formation, leading to alteration of its activity (38). β-Cells are highly vulnerable to oxidative stress that is a characteristic in type 2 diabetes (39). Because h-IAPP oligomers disrupt β-cell mitochondrial integrity (15), it is likely that h-IAPP contributes to β-cell oxidative stress (40) that is compounded by subsequent hyperglycemia. We conclude that h-IAPP oligomers may induce UCH-L1 deficiency by decreasing UCH-L1 gene expression and/or by the way of post-translational modifications mediated through oxidative damage.

Although we reproducibly demonstrated that h-IAPP induced UCH-L1 downregulation in different models, endogenous h-IAPP expression did not decrease proteasome activity. Proteasome activity was decreased in human islets incubated with applied exogenous h-IAPP (41). This discrepancy can be explained by the differences between exogenously applied h-IAPP (41) and endogenously expressed h-IAPP. Application of toxic protein oligomers extracellularly bypasses the ERAD/ubiquitin/proteasome system for removal of toxic oligomers as they are formed. The overwhelming actions of this approach induce apoptosis in most cells within 24 h (9). However, data are accumulating to suggest that toxic h-IAPP oligomers form intracellularly in some β-cells in type 2 diabetes (15) and have a more subtle effect on β-cell viability and function as described in animal models that develop diabetes through transgenic expression of h-IAPP (42).

The lack of an adverse effect of endogenously expressed h-IAPP on proteasome catalytic activity suggests that h-IAPP compromises the ubiquitin/proteasome system upstream of the proteasome. Because ubiquitinated proteins accumulate with increased h-IAPP, we considered that the ubiquitination process itself is unlikely to be perturbated. A more plausible explanation for accumulation of ubiquinated proteins with increased expression of h-IAPP is compromised delivery of ubiquitinated proteins to the proteasome. Degradation of proteins targeted for proteasomal degradation may be altered by abnormal modifications of substrates, per se, impairing their binding and/or recognition by the functional 20S proteasome. Thus, accumulation of ubiquitinated proteins may be a consequence of inhibition of deubiquitinating activity rather than direct effect on the proteasome (43). We hypothesized that in β-cells expressing h-IAPP, deficient UCH-L1 availability might lead to impaired polyubiquitin removal from proteins targeted for degradation before entry into the 20S proteasome, leading to the obstruction of the 20S pore by a forked substrate. Consistent with this hypothesis, we and others have demonstrated that inhibition of UCH-L1 led to accumulation of ubiquitinated proteins (27–29).

Modification of a protein with ubiquitin chains is the hallmark of protein degradation by the proteasome. However, recent data imply a role for ubiquitin in lysosome-dependent degradation, known as autophagy (44). In rodent β-cells, defects in autophagy are associated with accumulation of polyubiquitinated proteins (45–47). Also, β-cells in type 2 diabetes show evidence of altered autophagy (48). Interestingly, the intracellular storage of ubiquitinated aggregates in patients with lysosomal storage disorders is associated with deficiency of UCH-L1 (28). Recently, the p62/autophagy/lysosomal degradation system, an alternative mechanism to clear ubiquinated proteins, was shown to be compromised by high expression of h-IAPP (32). Given the approximately 40% decreased availability of UCH-L1 protein (and possibly further decreased function through post-translational modifications, vida supra) and impaired autophagy in β-cells in type 2 diabetes (48), both major pathways for removal of misfolded proteins are dysfunctional. Moreover, the rate of formation of misfolded proteins per β-cell requiring degradation is likely increased given the conditions of insulin resistance and decreased β-cell number as well as compromised ER function arising from ER stress and disrupted ER Ca^{2+} homeostasis induced by membrane permeant oligomers (15,33) and glucolipotoxicity.

Arguments in favor of a relatively early role of impaired β-cell protein homeostasis include the early presence of impaired β-cell function that precedes type 2 diabetes (49), reproduced in the HIP rat (14). However, increased expression of h-IAPP upon obesity is insufficient alone to explain why ~20% of individuals with morbid obesity develop type 2 diabetes, whereas 80% do not. The contributor factors that may explain this include variance between individuals in the efficiency of protein chaperoning through the secretory pathway and variance in the β-cell mass accomplished during postnatal expansion. The latter results in a wide range of β-cell mass in young adults (50) and therefore presumably β-cell synthetic burden in individuals that subsequently become obese.

Because elimination of misfolded proteins is important for cell viability, we investigated the effects of UCH-L1 availability on β-cell viability. High expression of h-IAPP induces β-cell apoptosis through the mechanism of ER stress (1,16), but the precise molecular events triggering ER stress are unknown. Here, we show that increased expression of h-IAPP (but not r-IAPP) decreased UCH-L1 levels and that loss of UCH-L1 expression and activity induced ER stress and apoptosis in β-cells. Therefore, increased h-IAPP expression induces ER stress and β-cell apoptosis that is mediated, at least in part, by abnormal function of UCH-L1. In addition, the accumulation of ubiquitinated proteins might also exacerbate ER stress

(51). It is likely that the tipping point from compromised β-cell function to β-cell apoptosis is driven by this unsustainable cycle once UCH-L1 function and the back up pathway of autophagy are attenuated.

In summary, we report that β-cells in type 2 diabetes share the characteristics of affected neurons in Alzheimer's and Parkinson's diseases with attenuated UCH-L1 protein levels and accumulation of ubiquitin conjugates. Increased expression of h-IAPP in β-cells, as occurs in insulin resistant states such as obesity, can lead to the formation of h-IAPP toxic oligomers and accumulation of polyubiquitinated proteins associated with decreased UCH-L1 availability. Downregulation of UCH-L1 expression and activity in β-cells induces ER stress and apoptosis. We conclude that a defective protein degradation system in β-cells in type 2 diabetes can, at least in part, be attributed to misfolded h-IAPP leading to UCH-L1 deficiency, which in turn further compromises β-cell viability.

ACKNOWLEDGMENTS

These studies were supported by grants from the National Institutes of Health (DK059579) and the Larry L. Hillblom Foundation (2007-D-003-NET and 2008-D-027-FEL [to S.C.]).

No potential conflicts of interest relevant to this article were reported.

S.C. designed and performed the experiments and wrote the manuscript. C.-j.H., T.G., M.D., A.V.M., R.A.R., and A.E.B. contributed to the experiments and reviewed/edited the manuscript. P.C.B. contributed to the discussion and wrote, reviewed, and edited the manuscript.

We thank Chang Liu, Heather Cox, and Ryan Galasso at the Larry Hillblom Islet Research Center for their excellent technical help.

REFERENCES

1. Huang CJ, Lin CY, Haataja L, Gurlo T, Butler AE, Rizza RA, Butler PC. High expression rates of human islet amyloid polypeptide induce endoplasmic reticulum stress-mediated β-cell apoptosis, a characteristic of humans with type 2 but not type 1 diabetes. Diabetes 2007;56:2016–2027
2. Marchetti P, Bugliani M, Lupi R, Marselli L, Masini M, Boggi U, Filipponi F, Weir GC, Eizirik DL, Cnop M. The endoplasmic reticulum in pancreatic beta cells of type 2 diabetes patients. Diabetologia 2007;50:2486–2494
3. Butler AE, Janson J, Bonner-Weir S, Ritzel R, Rizza RA, Butler PC. β-Cell deficit and increased β-cell apoptosis in humans with type 2 diabetes. Diabetes 2003;52:102–110
4. Laybutt DR, Preston AM, Akerfeldt MC, Kench JG, Busch AK, Biankin AV, Biden TJ. Endoplasmic reticulum stress contributes to beta cell apoptosis in type 2 diabetes. Diabetologia 2007;50:752–763
5. Kloppel G, Lohr M, Habich K, Oberholzer M, Heitz PU. Islet pathology and the pathogenesis of type 1 and type 2 diabetes mellitus revisited. Surv Synth Pathol Res 1985;4:110–125
6. Matveyenko AV, Gurlo T, Daval M, Butler AE, Butler PC. Successful versus failed adaptation to high-fat diet-induced insulin resistance: the role of IAPP-induced β-cell endoplasmic reticulum stress. Diabetes 2009;58:906–916
7. Mulder H, Ahren B, Stridsberg M, Sundler F. Non-parallelism of islet amyloid polypeptide (amylin) and insulin gene expression in rats islets following dexamethasone treatment. Diabetologia 1995;38:395–402
8. Butler PC, Chou J, Carter WB, Wang YN, Bu BH, Chang D, Chang JK, Rizza RA. Effects of meal ingestion on plasma amylin concentration in NIDDM and nondiabetic humans. Diabetes 1990;39:752–756
9. Haataja L, Gurlo T, Huang CJ, Butler PC. Islet amyloid in type 2 diabetes, and the toxic oligomer hypothesis. Endocr Rev 2008;29:303–316
10. Butler AE, Jang J, Gurlo T, Carty MD, Soeller WC, Butler PC. Diabetes due to a progressive defect in β-cell mass in rats transgenic for human islet amyloid polypeptide (HIP rat): a new model for type 2 diabetes. Diabetes 2004;53:1509–1516
11. Butler AE, Janson J, Soeller WC, Butler PC. Increased β-cell apoptosis prevents adaptive increase in β-cell mass in mouse model of type 2 diabetes: evidence for role of islet amyloid formation rather than direct action of amyloid. Diabetes 2003;52:2304–2314
12. Hoppener JWM, Oosterwijk C, Nieuwenhuis MG, Posthuma G, Thijssen JHH, Vroom TM, Ahren B, Lips CJM. Extensive islet amyloid formation is induced by development of type II diabetes mellitus and contributes to its progression: pathogenesis of diabetes in a mouse model. Diabetologia 1999;42:427–434
13. Janson J, Soeller WC, Roche PC, Nelson RT, Torchia AJ, Kreutter DK, Butler PC. Spontaneous diabetes mellitus in transgenic mice expressing human islet amyloid polypeptide. Proc Natl Acad Sci U S A 1996;93:7283–7288
14. Matveyenko AV, Butler PC. β-Cell deficit due to increased apoptosis in the human islet amyloid polypeptide transgenic (HIP) rat recapitulates the metabolic defects present in type 2 diabetes. Diabetes 2006;55:2106–2114
15. Gurlo T, Ryazantsev S, Huang CJ, Yeh MW, Reber HA, Hines OJ, O'Brien TD, Glabe CG, Butler PC. Evidence for proteotoxicity in beta cells in type 2 diabetes: toxic islet amyloid polypeptide oligomers form intracellularly in the secretory pathway. Am J Pathol 2010;176:861–869
16. Huang CJ, Haataja L, Gurlo T, Butler AE, Wu XJ, Soeller WC, Butler PC. Induction of endoplasmic reticulum stress-induced beta-cell apoptosis and accumulation of polyubiquitinated proteins by human islet amyloid polypeptide. Am J Physiol Endocrinol Metab 2007;293:E1656–E1662
17. Meusser B, Hirsch C, Jarosch E, Sommer T. ERAD: the long road to destruction. Nat Cell Biol 2005;7:766–772
18. Hershko A, Ciechanover A. The ubiquitin system. Annu Rev Biochem 1998;67:425–479
19. Stefani M. Protein misfolding and aggregation: new examples in medicine and biology of the dark side of the protein world. Biochim Biophys Acta 2004;1739:5–25
20. Lam YA, Pickart CM, Alban A, Landon M, Jamieson C, Ramage R, Mayer RJ, Layfield R. Inhibition of the ubiquitin-proteasome system in Alzheimer's disease. Proc Natl Acad Sci U S A 2000;97:9902–9906
21. McNaught KSP, Jenner P. Proteasomal function is impaired in substantia nigra in Parkinson's disease. Neurosci Lett 2001;297:191–194
22. Waelter S, Boeddrich A, Lurz R, Scherzinger E, Lueder G, Lehrach H, Wanker EE. Accumulation of mutant huntingtin fragments in aggresome-like inclusion bodies as a result of insufficient protein degradation. Mol Biol Cell 2001;12:1393–1407
23. Rubinsztein DC. The roles of intracellular protein-degradation pathways in neurodegeneration. Nature 2006;443:780–786
24. Choi J, Levey AI, Weintraub ST, Rees HD, Gearing M, Chin LS, Li L. Oxidative modifications and down-regulation of ubiquitin carboxyl-terminal hydrolase L1 associated with idiopathic Parkinson's and Alzheimer's diseases. J Biol Chem 2004;279:13256–13264
25. Lopez-Avalos MD, Duvivier-Kall VF, Xu G, Bonner-Weir S, Sharma A, Weir GC. Evidence for a role of the ubiquitin-proteasome pathway in pancreatic islets. Diabetes 2006;55:1223–1231
26. Wilkinson KD, Lee KM, Deshpande S, Duerksen-Hughes P, Boss JM, Pohl J. The neuron-specific protein PGP 9.5 is a ubiquitin carboxyl-terminal hydrolase. Science 1989;246:670–673
27. Tan YY, Zhou HY, Wang ZQ, Chen SD. Endoplasmic reticulum stress contributes to the cell death induced by UCH-L1 inhibitor. Mol Cell Biochem 2008;318:109–115
28. Bifsha P, Landry K, Ashmarina L, Durand S, Seyrantepe V, Trudel S, Quiniou C, Chemtob S, Xu Y, Gravel RA, Sladek R, Pshezhetsky AV. Altered gene expression in cells from patients with lysosomal storage disorders suggests impairment of the ubiquitin pathway. Cell Death Differ 2007;14:511–523
29. Saigoh K, Wang YL, Suh JG, Yamanishi T, Sakai Y, Kiyosawa H, Harada T, Ichihara N, Wakana S, Kikuchi T, Wada K. Intragenic deletion in the gene encoding ubiquitin carboxy-terminal hydrolase in gad mice. Nat Genet 1999;23:47–51
30. Hohmeier HE, Mulder H, Chen GX, Henkel-Rieger R, Prentki M, Newgard CB. Isolation of INS-1–derived cell lines with robust ATP-sensitive K+ channel-dependent and -independent glucose-stimulated insulin secretion. Diabetes 2000;49:424–430
31. Costes S, Broca C, Bertrand G, Lajoix AD, Bataille D, Bockaert J, Dalle S. ERK1/2 control phosphorylation and protein level of cAMP-responsive element-binding protein: a key role in glucose-mediated pancreatic β-cell survival. Diabetes 2006;55:2220–2230
32. Rivera JF, Gurlo T, Daval M, Huang CJ, Matveyenko AV, Butler PC, Costes S. Human-IAPP disrupts the autophagy/lysosomal pathway in pancreatic beta-cells: protective role of p62-positive cytoplasmic inclusions. Cell Death Differ 2010 [Epub ahead of print]
33. Huang CJ, Gurlo T, Haataja L, Costes S, Daval M, Ryazantsev S, Wu XJ, Butler AE, Butler PC. Calcium-activated calpain-2 is a mediator of beta cell

dysfunction and apoptosis in type 2 diabetes. J Biol Chem 2010;285:339–348
34. Coux O, Tanaka K, Goldberg AL. Structure and functions of the 20S and 26S proteasomes. Annu Rev Biochem 1996;65:801–847
35. Borodovsky A, Ovaa H, Kolli N, Gan-Erdene T, Wilkinson KD, Ploegh HL, Kessler BM. Chemistry-based functional proteomics reveals novel members of the deubiquitinating enzyme family. Chem Biol 2002;9:1149–1159
36. Kagara I, Enokida H, Kawakami K, Matsuda R, Toki K, Nishimura H, Chiyomaru T, Tatarano S, Itesako T, Kawamoto K, Nishiyama K, Seki N, Nakagawa M. CpG hypermethylation of the UCHL1 gene promoter is associated with pathogenesis and poor prognosis in renal cell carcinoma. J Urol 2008;180:343–351
37. Bartoszewski R, Rab A, Twitty G, Stevenson L, Fortenberry J, Piotrowski A, Dumanski JP, Bebok Z. The mechanism of cystic fibrosis transmembrane conductance regulator transcriptional repression during the unfolded protein response. J Biol Chem 2008;283:12154–12165
38. Kabuta T, Setsuie R, Mitsui T, Kinugawa A, Sakurai M, Aoki S, Uchida K, Wada K. Aberrant molecular properties shared by familial Parkinson's disease-associated mutant UCH-L1 and carbonyl-modified UCH-L1. Hum Mol Genet 2008;17:1482–1496
39. Robertson RP. Chronic oxidative stress as a central mechanism for glucose toxicity in pancreatic islet beta cells in diabetes. J Biol Chem 2004;279:42351–42354
40. Zraika S, Hull RL, Udayasankar J, Aston-Mourney K, Subramanian SL, Kisilevsky R, Szarek WA, Kahn SE. Oxidative stress is induced by islet amyloid formation and time-dependently mediates amyloid-induced beta cell apoptosis. Diabetologia 2009;52:626–635
41. Casas S, Gomis R, Gribble FM, Altirriba J, Knuutila S, Novials A. Impairment of the ubiquitin-proteasome pathway is a downstream endoplasmic reticulum stress response induced by extracellular human islet amyloid polypeptide and contributes to pancreatic β-cell apoptosis. Diabetes 2007;56:2284–2294
42. Lin CY, Gurlo T, Kayed R, Butler AE, Haataja L, Glabe CG, Butler PC. Toxic human islet amyloid polypeptide (h-IAPP) oligomers are intracellular, and vaccination to induce anti-toxic oligomer antibodies does not prevent h-IAPP-induced β-cell apoptosis in h-IAPP transgenic mice. Diabetes 2007;56:1324–1332
43. Koulich E, Li X, DeMartino GN. Relative structural and functional roles of multiple deubiquitylating proteins associated with mammalian 26S proteasome. Mol Biol Cell 2008;19:1072–1082
44. Kirkin V, McEwan DG, Novak I, Dikic I. A role for ubiquitin in selective autophagy. Mol Cell 2009;34:259–269
45. Ebato C, Uchida T, Arakawa M, Komatsu M, Ueno T, Komiya K, Azuma K, Hirose T, Tanaka K, Kominami E, Kawamori R, Fujitani Y, Watada H. Autophagy is important in islet homeostasis and compensatory increase of beta cell mass in response to high-fat diet. Cell Metab 2008;8:325–332
46. Jung HS, Chung KW, Won Kim J, Kim J, Komatsu M, Tanaka K, Nguyen YH, Kang TM, Yoon KH, Kim JW, Jeong YT, Han MS, Lee MK, Kim KW, Shin J, Lee MS. Loss of autophagy diminishes pancreatic beta cell mass and function with resultant hyperglycemia. Cell Metab 2008;8:318–324
47. Kaniuk NA, Kiraly M, Bates H, Vranic M, Volchuk A, Brumell JH. Ubiquitinated-protein aggregates form in pancreatic β-cells during diabetes-induced oxidative stress and are regulated by autophagy. Diabetes 2007;56:930–939
48. Masini M, Bugliani M, Lupi R, del Guerra S, Boggi U, Filipponi F, Marselli L, Masiello P, Marchetti P. Autophagy in human type 2 diabetes pancreatic beta cells. Diabetologia 2009;52:1083–1086
49. Weyer C, Bogardus C, Mott DM, Pratley RE. The natural history of insulin secretory dysfunction and insulin resistance in the pathogenesis of type 2 diabetes mellitus. J Clin Invest 1999;104:787–794
50. Meier JJ, Butler AE, Saisho Y, Monchamp T, Galasso R, Bhushan A, Rizza RA, Butler PC. β-Cell replication is the primary mechanism subserving the postnatal expansion of β-cell mass in humans. Diabetes 2008;57:1584–1594
51. Paschen W. Endoplasmic reticulum: a primary target in various acute disorders and degenerative diseases of the brain. Cell Calcium 2003;34:365–383